RPN46

ION ACCELERATION WITH HIGH ν/γ ELECTRON BEAMS*

PIIR-9-70

December 1969

by

J. Rander, B. Ecker, and G. Yonas

Physics International Company
2700 Merced Street
San Leandro, California 94577

*Presented in part as "Observation of Particles Accelerated by Intense Electron Streams" at the Meeting of the Division of Plasma Physics, American Physical Society, November 1969, Los Angeles.

CONTENTS

ILLUSTRATIONS

SECTION I

INTRODUCTION

With the observation of electron-beam-accelerated MeV-ions by Ion Physics Corporation last year (Reference 1), considerable interest has been generated over the process. Last spring, a small research group was formed at Physics International and work was begun on a series of exploratory measurements (Reference 2 and 3). In the most recent experiments, measurements were made to allow some correlation between the physics of the electron beam and ion acceleration.

In addition to the process of acceleration, we were interested in understanding the capabilities of low-energy, very high-current electron beams to provide suitable acceleration conditions. The possibility of a strong current dependence, as observed by Graybill and Uglum (Reference 1) and as suggested theoretically by Putnam (Reference 4), indicated that an economical accelerator approach might be found in these low-energy, high-current beams.

SECTION II

EXPERIMENTAL PROCEDURE

Basically, the experiments consisted of injecting a pulsed electron beam into a gas-filled drift chamber. Ions formed and accelerated in the chamber were analyzed downstream (Figure 1). The details of this apparatus have been described in Reference 3. The net current was measured in the drift region with four Rogowski coils. The ions formed and accelerated in the drift chamber, along with the remnant of the electron beam, were transported into an evacuated region where the electrons were removed with a sweeping magnet. The ions were then observed with current collectors, passed through a collimator, momentum analyzed in a magnet, and finally collected on nuclear emulsion plates. The nuclear emulsions, combined with momentum information from the magnet, formed our principle ion-detection technique.

The experiments were performed with beams of 250 keV to 1 MeV mean electron energy and corresponding peak diode currents of 200 to 100 kA.* Pressure in the drift region typically was 200 μ for hydrogen and helium and 20 μ for nitrogen and argon.

---

*The PI 738 Pulserad facility was used for these two experiments and is described in Reference 5.

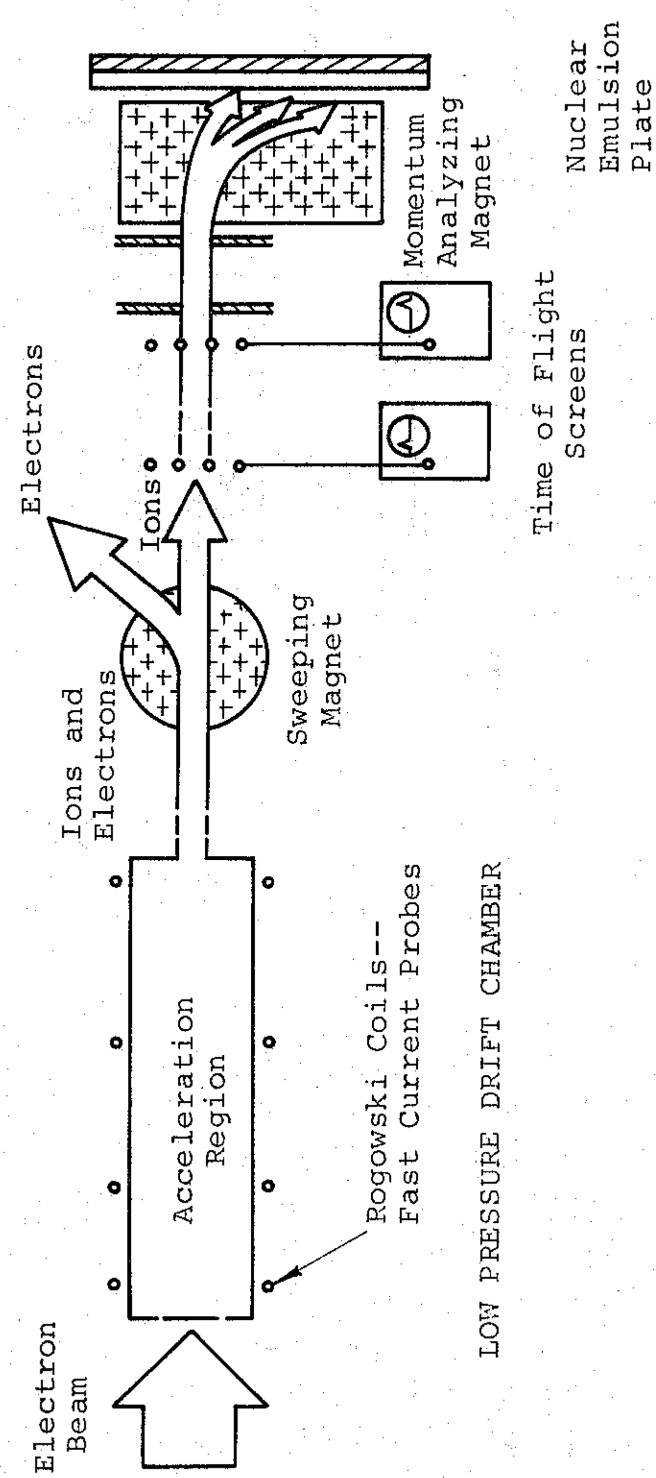

FIGURE 1. APPARATUS

8479

SECTION III

RESULTS AND DISCUSSION

Figures 2 and 3 present nuclear emulsion data for hydrogen and helium drift gases. The particles in both cases were identified by requiring agreement between range and momentum information. In Figure 2, a selection of photomicrographs of the emulsion plate for a 250 keV pulse in hydrogen and the corresponding proton momentum spectrum are shown. From the track densities, one can resolve the momentum peak. The narrow peak width is consistent with our collimator resolution and represents an energy spread of $\leq$ 15% FWHM at 840 keV. Time-of-flight data indicate a second peak with a momentum of 32 MeV/cm but this fell below the spectrometer cut-off.

Figure 3 shows similar data for a 650-keV pulse in helium. The photomicrographs show the differences in range which were observed for various particles. (This pulse did not have the usual multiple energy peaks.) The clear dependence of ion energy on charge is evident--we have 1.8 MeV protons and helium^{+1} ions, and 3.6 MeV helium^{+2} ions. The momentum spreads are again consistent with our resolution. (The presence of protons on this pulse in which the drift gas was helium is presumably due to outgassing of considerable amounts of water from the nuclear emulsion.)

Similar pulsing in nitrogen and argon also shows a linear dependence of ion energy upon charge (Figure 4). We have observed a linear dependence over the range from 1 to 40 times the proton mass and from one to six times the charge, which is in agreement with the time-of-flight measurements of Graybill and Uglum (Reference 1).

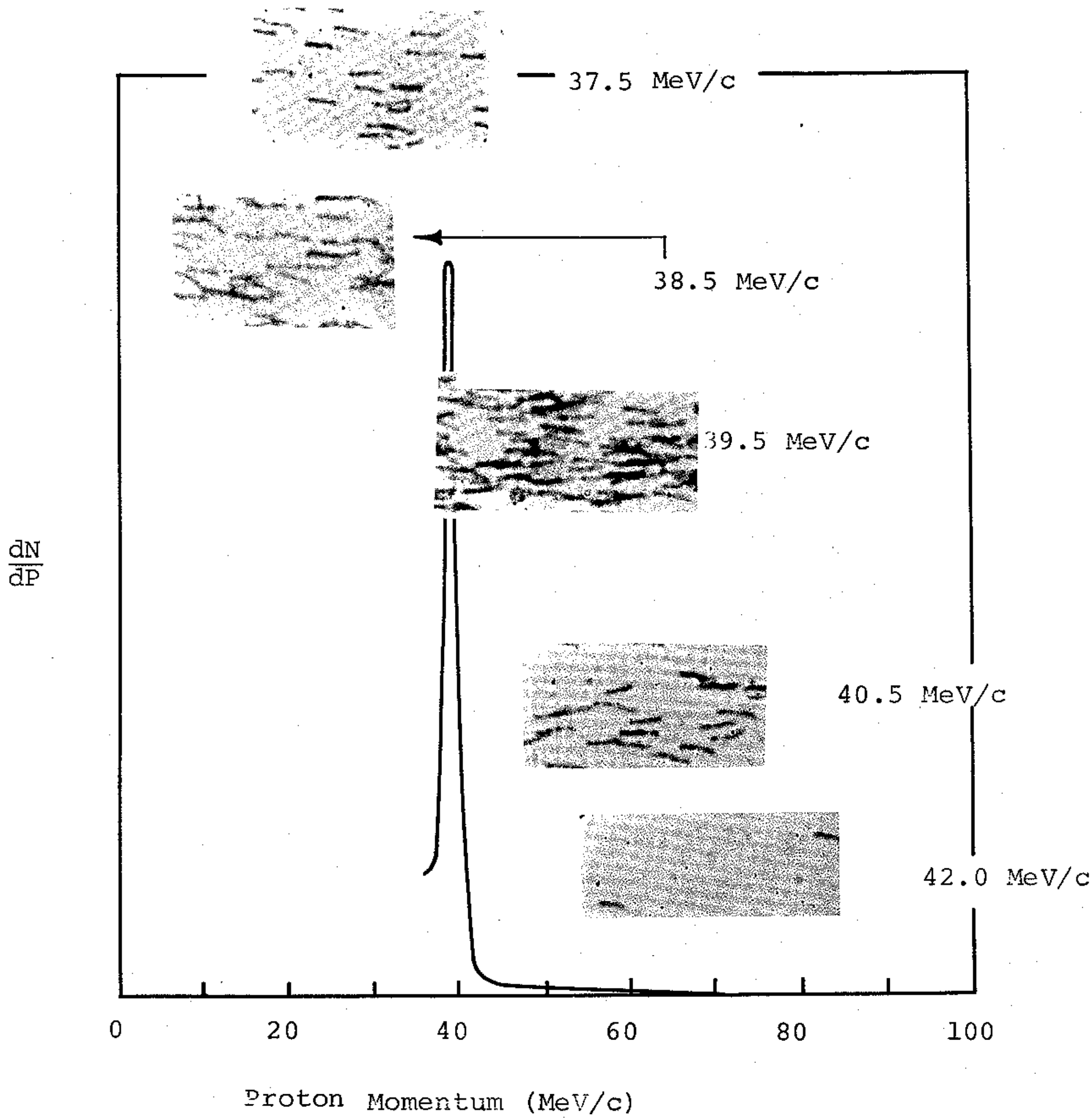

FIGURE 2. H_2 PULSE--NUCLEAR EMULSION DATA

8316

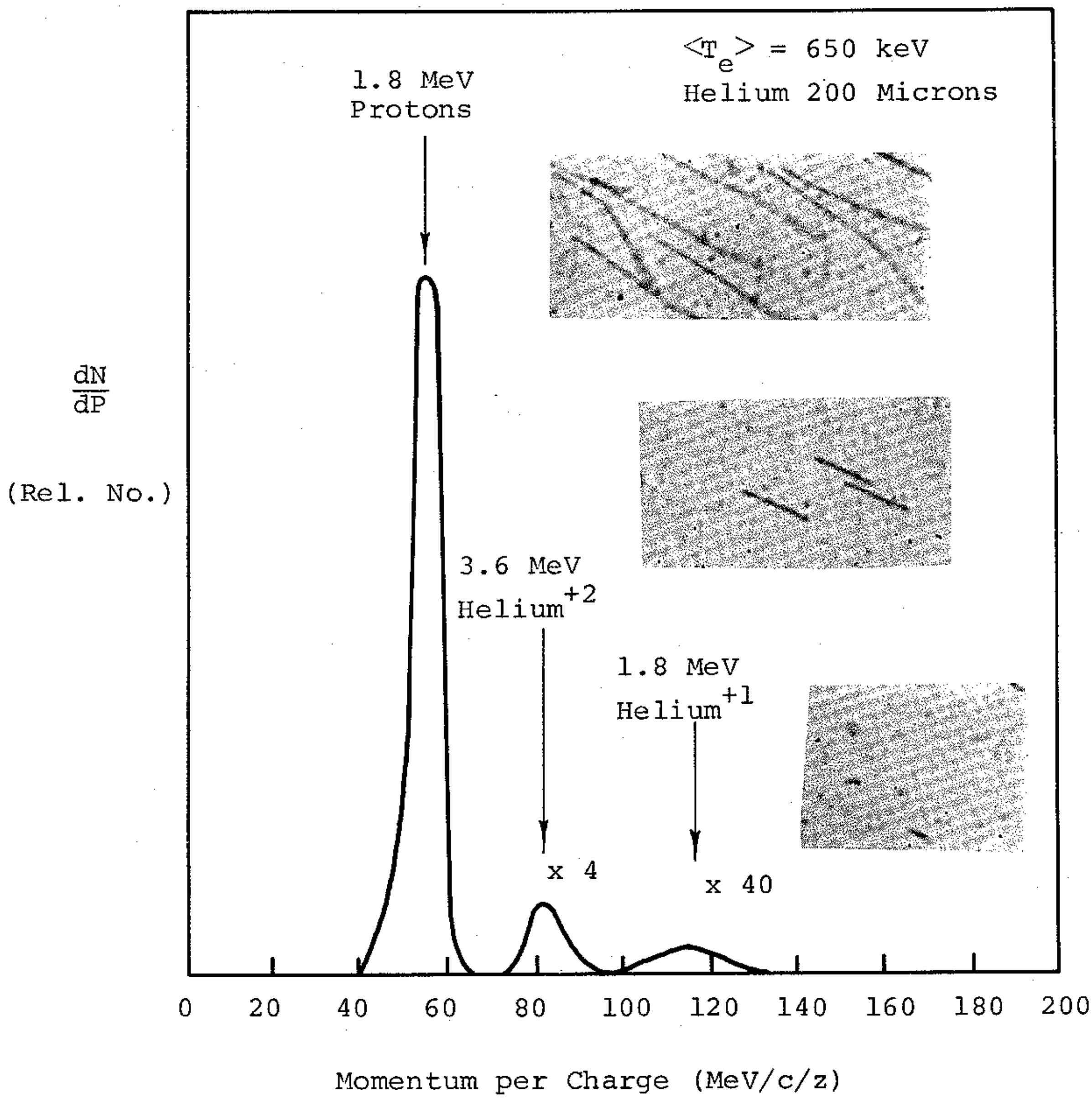

FIGURE 3. He PULSE--NUCLEAR EMULSION DATA

8294

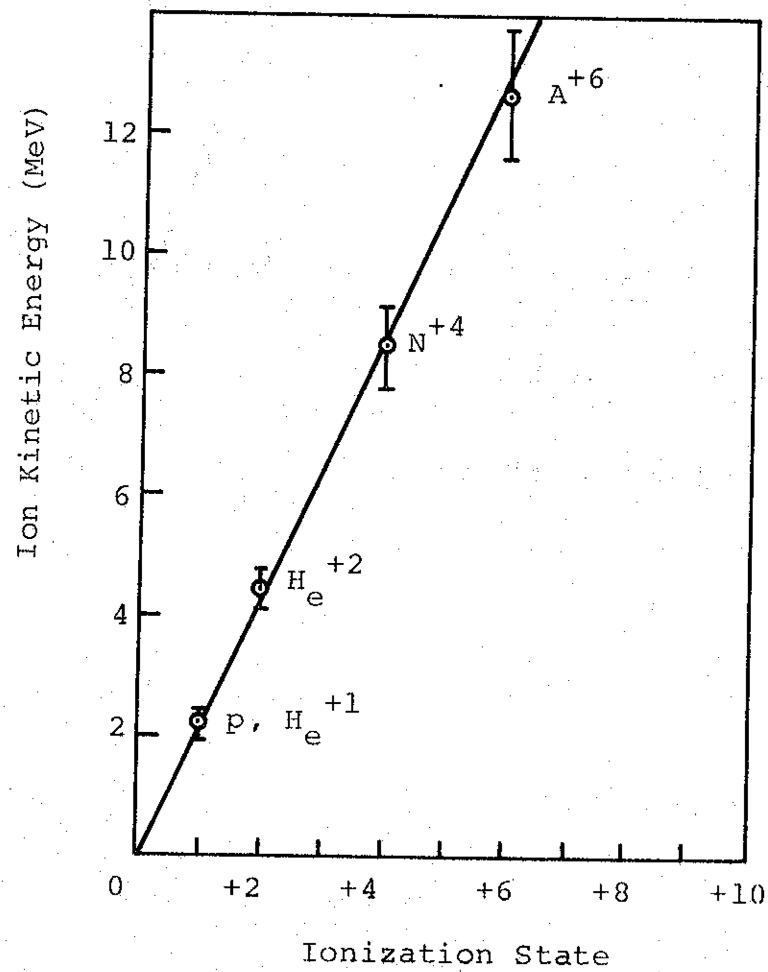

FIGURE 4. LINEAR DEPENDENCE OF ION ENERGY ON CHARGE

8293

To understand the properties of high-current, low-energy electron beams in this process, we performed an energy-current scan from 250 keV to 1 MeV and from 200 to 100 kA. Displayed in Figure 5 are the number of pulses with a maximum proton energy in a 200 keV wide bin. The value of ν/γ given is a rough measure of the ratio of the transverse to longitudinal energy components in the electron beam.

From this survey, we can make two observations: First, as the electron energy is increased, and the current lowered, we observe that the acceleration process becomes much more reproducible, i.e., we note a decrease in the scatter of maximum proton energies as ν/γ is reduced. Second, we observe a shift in the mean proton energy from 1.65 ± 0.35 MeV at 650 keV, to 2.03 ± 0.18 MeV at 1 MeV mean electron energy. This shift in energy may be due to the difference in electron beam energy. The data of Graybill and Uglum (Reference 1) and theoretical studies by Putnam (Reference 4), however, emphasize current dependences so both the diode current profiles and the net current in the drift chamber were examined (Figure 6). It was observed that the 650 keV diode current is larger than the 1 MeV case and as such can not explain the ion energy difference. The net current, however, shows that for the first 10 nsec or so the 1 MeV beam produces a higher net current. The onset of acceleration occurs at the first peak in the net current profiles, about 7 nsec after t = 0. If the shift in energies is due primarily to net current variations, then it appears that there is a strong current dependence.

Using fast current probes, the time of flight was measured for the electron beam front in the drift chamber. Figure 7 shows the data for 250 and 650 keV beams. We typically observe a delay of 5 to 30 nsec wherein the beam front hovers within 5 cm of the

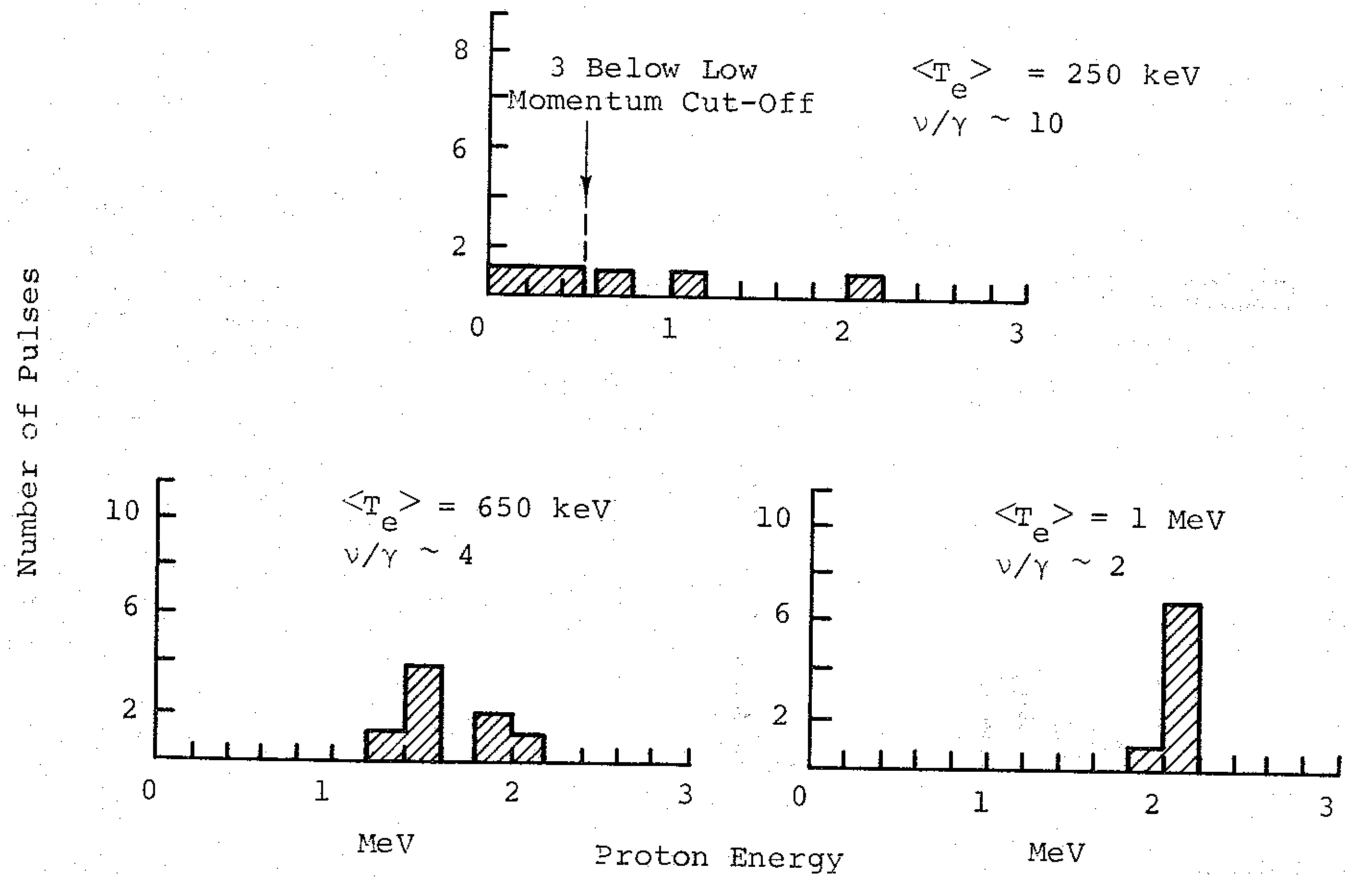

FIGURE 5. MAXIMUM PROTON ENERGY OBTAINED PER PULSE

8477

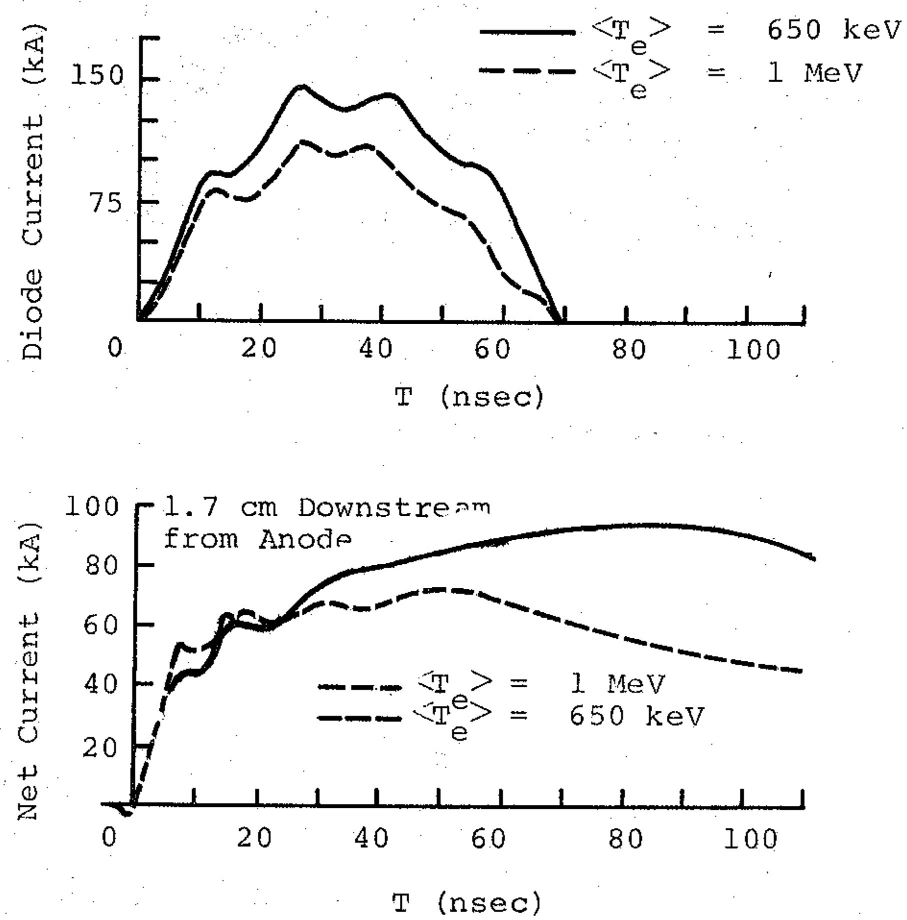

FIGURE 6. PARTICLE ENERGY--CURRENT DEPENDENCE

8291

anode after first being introduced into the chamber. This time appears to be related to obtaining a balance between space charge and the magnetic forces of the beam. Using a simple model assuming only collisional ionization, this time can be expressed as

$$t = \frac{1}{n\sigma\beta\gamma^2 c}$$

where n = drift gas number density, σ = ionization cross-section, and β,γ refer to the mean electron energies. At this time, the ratio of ions to electrons is $1/\gamma^2$. After this balance is achieved the beam front velocity increases. It is just at this moment that we observe the beginning of ion acceleration using time-of-flight data. (The shift in this time from 250 keV to 650 keV is due to the difference in $1/\beta\gamma^2$ in the expression above.) This is the same delay Graybill and Uglum subtracted from their proton timing data to obtain straight-line fits for different gas pressures (Reference 1).

We attempted to alter the process by changing both the drift pipe diameter and the cathode geometry. Cathodes were used that gave either a solid or hollow electron stream in the first 20 nsec. No significant change was observed, either in maximum proton energy or in multiple energy peak positions. Figure 8 presents cases where both cathode geometry and pipe diameter were varied simultaneously. There were no large shifts of either the first or second peak.

Summarizing all of our data the following observation can be made:

1. Particles from protons through argon ions have been accelerated.

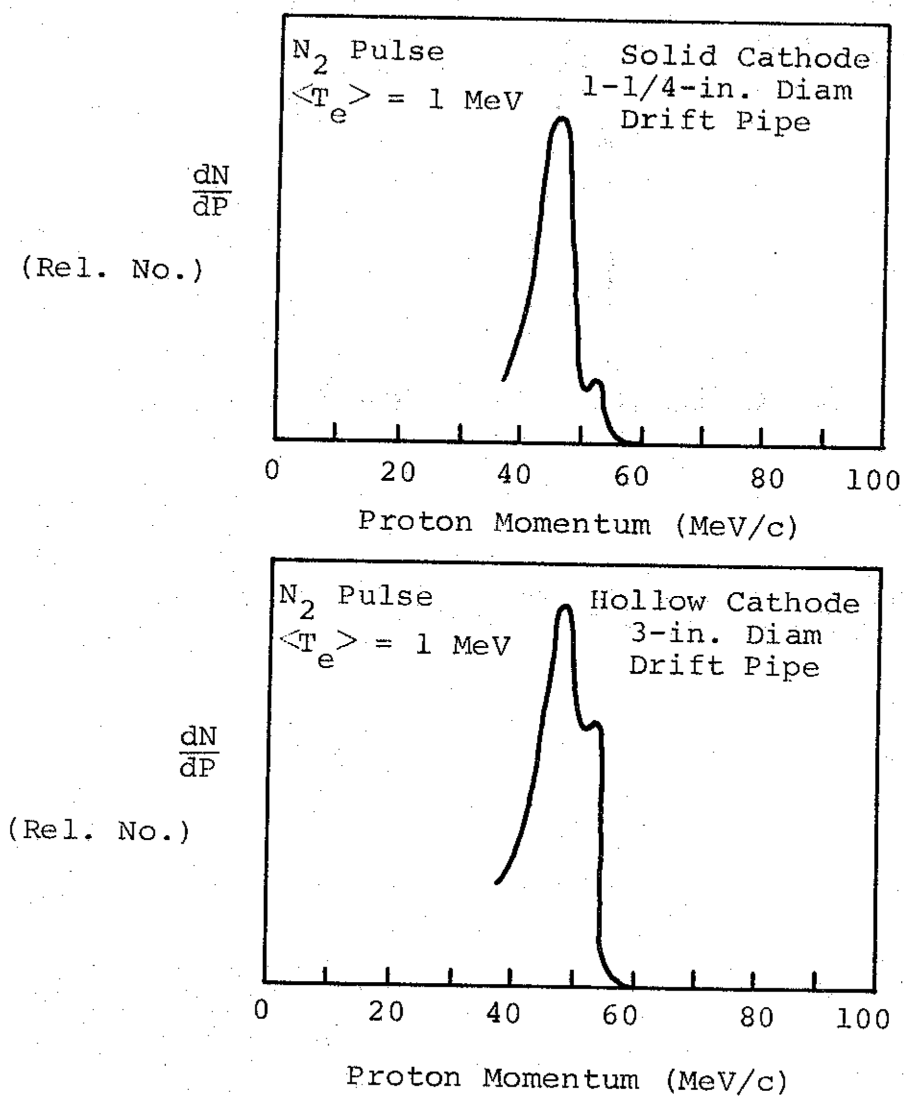

FIGURE 8. PROTON SPECTRA WITH DIFFERENT INJECTION AND DRIFT GEOMETRIES

2. Particle energy depends linearly upon charge.

3. The energy per charge is not strongly dependent upon drift gas or pressure.

4. The particle energy becomes more reproducible with higher energy, lower current beams.

5. The energy is insensitive to drift pipe diameter or injection conditions, i.e., hollow-solid cathodes.

6. The proton energy peak widths are ≤ 15 ~ 20% FWHM (consistent with our limits of resolution).

7. Multiple energy peaks are observed with our beam.

8. The beam front begins to propagate and ions are accelerated when force neutralization occurs ($t \approx \frac{1}{n\sigma\beta\gamma^2 c}$).

9. Fluxes of 10^{12} to 10^{14} particles, assuming production into a steradian, are accelerated per beam pulse.

Concerning the use of high ν/γ beams, we found that energy reproducibility suffered with higher ν/γ. Further, we found that high diode currents do not translate directly into correspondingly high net currents at the time when acceleration occurs.

REFERENCES

1. S. E. Graybill and J. R. Uglum, Ion Physics Corp., Internal Report 903-TR-355 (1969).

2. G. Yonas, P. Spence, B. Ecker, and J. Rander, PIFR-106-2, Physics International Co., San Leandro, California, August 1969.

3. J. Rander, B. Ecker, G. Yonas, and D. Drickey, PITR-69-7, Physics International Co., San Leandro, California, September 1969; also joint preprint with Univ. of California, Los Angeles, UCLA-1043. (Submitted to Phys. Rev. Letters.)

4. S. Putnam, Paper presented at Meeting of the Division of Plasma Physics, American Physical Society, November 1969; Los Angeles, California.

5. G. Yonas and P. Spence, PIFR-106, Physics International Co., San Leandro, California, October 1968; DASA Contract 2175.